Catalysis Today 151 (2010) 2–7

Contents lists available at ScienceDirect

Catalysis Today

journal homepage: www.elsevier.com/locate/cattod

Innovative self-cleaning and bactericide textiles

J. Kiwi, C. Pulgarin

Ecole Polytechnique Fédéral de Lausanne, EPFL-SB-ISIC-GGEC, Lausanne 1015 Switzerland

ARTICLE INFO

Article history:
Available online 29 March 2010

Keywords:
Surface activation
Bactericide textiles
RF-plasma
Vacuum-UV pretreatment
DC-magnetron sputtering

ABSTRACT

To prepare bactericide textiles, TiO_2 has been added in the form of colloid, powder or a combination of both and the TiO_2 modified textiles subsequently cured at temperatures adapted to their specific heat resistance. The bactericide textile is activated and Ag is deposited on the activated cotton or polyester to induce oxygen functionalities containing diverse polar groups. These polar groups increase the bondability of TiO_2 and Ag with the textile surface. These functionalities generated in the presence of O_2 by RF-plasma (Radio-frequency plasma) and Vacuum-UV led to an increased adhesion of the TiO_2 and Ag on the textiles. Recent findings comprising surface chemistry, photochemistry and microbiology of the bactericide textiles are presented in detail.

1. Introduction

Self-cleaning by modified textile surfaces loaded with hydrophilic TiO_2 have been recently reported by Kiwi and co-workers [1–5]. RF-plasma and UVC has been used to activate textile and introduce oxygenated polar groups able to bond metal and oxides in a stable way on their surface. Daoud et al. have recently worked extensively on the deposition and testing of semiconductor and metallic deposits by state of the art methods to confer textiles diverse functionalities [6–10]. Radetic et al. [11] are pioneering the physical application of RF-plasma and corona discharge in self-cleaning and bactericide textiles. Montazer et al. [12,13] explored and characterized TiO_2 modified natural and artificial textiles. The EMPA laboratory [14–18] has recently reported the formation of metallic films on textiles pretreated by RF-plasma. Other recent significant contributions involving recent work in the textile sector have recently appeared [19–24].

The interest in using bactericide, anti-viral and fungicide textiles to treat skin diseases has significantly increased during the last several years. Bacteria have a low resistance to Ag, yet Ag is known to be benign to human cells. The recent progress in the deposition of Ag-nanoparticles on textiles has been a favorable development since a significant amount of Ag-clusters on the surface of textiles is exposed without hindrance to the surrounding medium. The Ag-deposition on cotton is important since cotton has the property to adsorb a large amount of moisture making this textile prone to microbial attack. With ambient temperature and humidity, cotton becomes a nutrient for bacterial and fungal growth.

RF-plasma activation of textiles imply the application of electromagnetic radiation at low P (0.1–1 Torr) since vacuum enhance the capture length of the electron and if residual O_2 is present this gas generates cations anions (O^-, O^+), radicals, excited sates, molecule-ions and electrons with high energy in a system where the local heat has a non-homogeneous distribution leading to a non equilibrium situation [1–3]. Experiments were almost carried out at low pressure when using RF-activation to enhance the capture length of the electron avoiding to a large degree due to collision deactivation. But recently pressures up to 1 atm have been used in conjunction with RF-plasma where the RF-plasma treatment has been used to generate localized heat effect [4,5]. In the RF-cavity intense local heat develops breaking H– and intermolecular bonds in cotton and Nylon. Intermolecular C–C bond scissions occur and the O_2 containing hydrophilic functional groups increase for polyester and wool-polyamide leading to improved wettability of these textiles [1]. In the presence of O_2, produce $-COO^-$, –O–O–, phenolic and lactam species develop on the textile surface as detected by XPS. By XPS it was possible to show the decrease in the C–C and C–H peaks at 285 eV due to the increase of COO^- and other carboxylic containing species. The increase of COO^- when RF-plasma activation was used lead to the release of CO_2. The concomitant formation of some benzenic species due to the RF-plasma suggests interaction between the textiles and the surface TiO_2 [4,5].

The RF-plasma in the presence of O_2 treatment roughens the textile surface leading to a better interaction between TiO_2 and the textile surface. Intermolecular C–C bond scissions occur and the oxygen containing hydrophilic functional groups increase for polyester and wool-polyamide leading to improved wettability of these textiles [1]. Recently, it has been reported that for polyester, the C–N and C–O the XPS peaks at 286.6 eV groups were doubled after corona discharge, whereas the peaks at 288.3 eV and 289.1 eV assigned to C=O and O–C=O groups also increased [25].

The light excitation at 185 nm does not have the energy content to produce cationic O^+ and anionic oxygen O^- species, as

0920-5861/$ – see front matter © 2010 Elsevier B.V. All rights reserved.
doi:10.1016/j.cattod.2010.01.032

it is the case of RF-plasma [1–2]. This light only leads to excited O*: O_2 Vacuum-UV → 2O*. The optical absorption between the light and the textile positioned at 3 mm of the light source at 1 atm air is very low. εO_2 (185 nm) = 2.6 M^{-1} cm^{-1} and εN_2 (185 nm) = 0.3 M^{-1} cm^{-1} at 185 nm/6.70 eV. Practically, no Vacuum-UV radiation is lost in the optical pathway between the light source and the cotton sample even at atmospheric pressures. TiO_2 modified cotton fabrics obtained by this pretreatment introduced surface activation with more evenly distributed than when activation by RF-plasma was used [4,5].

We describe recent work in this area focusing on four main areas: (a) RF-plasma activation of textile surfaces, (b) Vacuum-UV activation of textile surfaces (c) corrosion inhibition of textiles by SiO_2 as a binder and (d) bactericide Ag-textiles deposition by DC-magnetron sputtering.

2. Experimental

2.1. RF-plasma pretreatment of textile surfaces

The RF-plasma cavity from Harrick and Co, UK was applied with 100 W at 13.56 MHz. Different air pressures and times were set depending on the amount of O_2 desired during the pretreatment runs.

2.2. TiO_2-cotton pretreatment by Vacuum-UV

The Vacuum-UV light (a 25 W Hg lamp having 18 W at 254 nm and 7 W at 185 nm) to activate textiles was 70 cm long and had light sources with a diameter of 3 cm as shown in Fig. 3. Temperature in the cavity was 300–340 K depending on the reactor parameters combination.

2.3. X-ray photoelectron spectroscopy of TiO_2 modified cotton (XPS)

An AXIS NOVA photoelectron spectrometer (Kratos Analytical, Manchester, UK) equipped with monochromatic AlKα ($h\nu$ = 1486.6 eV) anode was used during the study. The kinetic energy of the photoelectrons was determined with the hemispheric analyzer set to the pass energy of 160 eV for wide-scan spectra and 20 eV for the case of high-resolution spectra. Electrostatic charge effect of the sample was overcompensated by means of the low-energy electron source working in combination with a magnetic immersion lens. Quantitative elemental compositions were determined from peak areas using experimentally determined sensitivity factors and spectrometer transmission function. Spectrum background was subtracted according to Shirley. The high-resolution spectra were analyzed by means of spectra deconvolution software (Vision 2, Kratos Analytical UK). In the XPS spectra, the Auger lines are identified along the XPS signals.

2.4. High-resolution transmission electron microscopy (HR TEM)

A Philips HR TEM CM 300 (field emission gun, 300 kV, 0.17 nm resolution) microscope and a Philips EM 430 (300 kV, LaB_6, 0.23 nm resolution) were used to measure the particles sizes of Ag-clusters. The textiles were embedded in epoxy resin (Embed 812) and the fabrics were cross-sectioned with an ultra-microtome (Ultracut E) to a thin section of 50–70 nm. Magnification from about 6800× to 41,000× was used to identify the Ag-clusters and determinate the Ag-layer thickness.

2.5. Ag-deposition on cotton by DC-magnetron sputtering

Fig. 6 shows the schematic diagram of the DC-magnetron sputtering. By using magnets behind the cathode to trap free electrons in the magnetic field, the probability of ionizing neutral gas atoms or molecules is enhanced by several orders of magnitude. The positive-ions near the target are accelerated towards the target surface by applying high negative voltages (0.2–2.0 kV). The Ag disk is eroded by Ar-ions and the ejected Ag-atoms/clusters/ions are collected on the cotton textile. An alloy of 1% Pt/Ag was employed to deposit the Ag/Pt on the cotton. The plasma working pressure was in the range of 0.1–1 Pa.

2.6. TiO_2 loading of cotton with TiO_2/SiO_2, details of CO_2 determination and light irradiation

The TiO_2 responsible for the self-cleaning effect through the production of highly oxidative radicals under band-gap irradiation is loaded on the textile in the following way: Immersion of the textile in a TiO_2 suspension of Degussa P-25 (or another variety of TiO_2), drying at 100 °C in vacuum oven, followed by sonication at 50–70 °C for 5–20 min to eliminate loosely bound TiO_2. The last three steps were repeated once more. A final heating of the textile was applied depending on the heat resistance limit of the textile followed by a short curing of the modified textile for 2–3 min at the temperature limit of the textile. This eliminates the residual condensation between the textile and the TiO_2 (TiOH in net sense) [26,27].

For the samples loaded with TiO_2/SiO_2 the cotton was dip-coated by TiO_2/SiO_2 sol–gel. The details of the preparation of the sol–gel solution have been previously reported [3]. Subsequently, moderate temperature treatment led to nanosized adhesive deposits.

The CO_2 was measured in a GC Carlo Erba 105 provided with a Poropak Q column. The wine stains wee applied on the cotton dropping 70 microliters red wine at 70 °C on the textile. The simulated sunlight irradiation of the samples was carried out in a Suntest cavity (Heraeus, Hanau, Germany) provided with a Xe-lamp calibrated at 50 mW/cm^2.

2.7. Airborne bacterial/fungi determination

The inactivation of bacteria and *fungi* of the cotton-Ag were evaluated in Petri dishes exposing the cotton samples of 1 cm^2 to air at room atmosphere for 2 h. Then, the samples were placed on an agar (Plate Count Agar, ref. 1.05463.0500 Merck) in a Petri dish ca. 9 cm diameter and were incubated in the absence of air for 24 h at 34 °C (±2 °C). Each determination was carried out in triplicate.

3. Results and discussions

3.1. Simulated sunlight discoloration of wine stains in TiO_2-cotton pretreated by RF-plasma

The colored pigments of wine sensitize the stain discoloration on cotton by the mechanism suggested in Fig. 1. The decomposi-

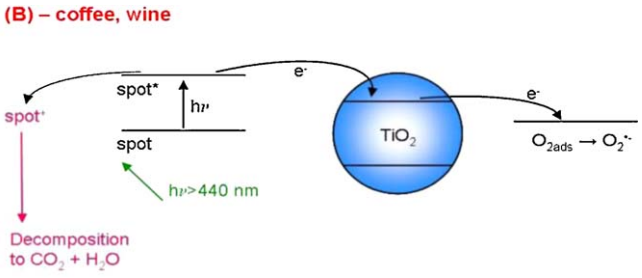

Fig. 1. Scheme of the self-cleaning mechanism of wine pigments on TiO_2-cotton pretreated by RF-plasma under sunlight-simulated light.

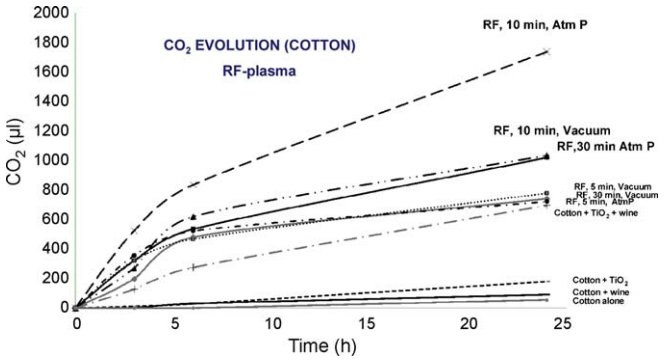

Fig. 2. Evolution of CO_2 during the wine stain discoloration as a function of irradiation time on cotton samples pretreated by RF-plasma.

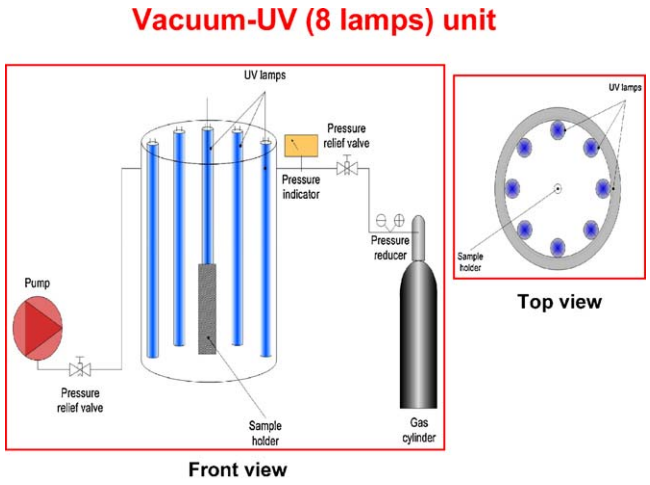

Fig. 3. Vacuum-UV unit with Hg-lamps (254 nm lamp, with 25% 185 nm radiation) used to pretreat the cotton textile.

tion of wine occurs due to photosensitization of the unstable cation under visible light excitation. This leads to the injection of an electron into the conduction band of TiO_2 as shown in Fig. 1 and in the presence of O_2 leads to O_2^- by the reaction $e^-_{cb} + O_2$ (ads) $\rightarrow O_2^-$. The decomposition of the wine stain also occurs by the by reaction of the wine stain (R*) with the TiO_2 photo-induced holes: $R^* + h^+_{vb} \rightarrow R^+ \rightarrow$ degradation products. The oxidative oxygenated radicals originating from O_2^- leads to long-lived intermediates that gradually decompose to carboxylic acids generating CO_2 as the final decomposition product through a photo-Kolbe type reaction: $RCOO^- + h^+_{vb} \rightarrow R^{\cdot} + CO_2$. The release of CO_2 is directly related to the oxidative decomposition of the wine and is accompanied by a small amount of cations and anions $C_xH_yN_vS_w$(-wine stain) + $H_2O_w + O_2 + h\nu \rightarrow CO_2 + H_2O + SO_p + NO_q$.

Fig. 2 shows the CO_2 evolution on the TiO_2-cotton pretreated by RF-plasma stained with red wine. The results in Fig. 2 show that at atmospheric pressure samples pretreated for 10 min decomposed giving rise to the largest amount of CO_2. Samples pretreated by RF-plasma without vacuum for 10 min produce the highest amount of CO_2 (1739 μl) after 24 h of irradiation. Samples pretreated by RF-plasma for 10 min showed a CO_2 evolution of 1036 μl, however, this quantity is very similar than that of the sample pretreated by RF at atmospheric pressure during 30 min (1022 μl). TiO_2-coated cotton stained with red wine but without any pretreatment by RF is shown in trace (c), the amount of CO_2 produced during 24 h of irradiation was low (698 μl). Furthermore, in control experiments very small amounts of CO_2 (55 μl) were observed when cotton was irradiated with daylight in the absence of TiO_2 and wine (trace a).

The reproducibility of the run with 10 min at 1 atm was repeated 5 times, adding each time 70 μl of red wine as describe din the experimental section. The results were reproducible in the range of 10% showing the stability of the discoloration performance of the TiO_2 modified cotton.

3.2. XPS studies of the Ti 2p peak during wine discoloration

Fig. 4 shows the XPS for samples stained with red wine as a function of the irradiation time. The XPS Ti2p peak signal of the cotton that was previously pretreated by Vacuum-UV (unit shown in Fig. 3) significantly changes the XPS spectra as the simulated sunlight was applied within 24 h. The most striking observation is that the 30–40 nm wine particles addition of wine to the cotton attenuated considerably the signal of the Ti2p peak at time zero (upper peak). It is noticed that Ti2p peaks grows significantly after 3 h of oxidation reaction. This indicates that after 3 h exposition significant removal of wine deposit (stain) took place. After 24 h of reaction Ti signal reaches around 70% of initial intensity indicating an advanced degree of destruction of the wine stain. Also the Ti2p3/2 peak shifts (not shown in Fig. 4) from 458.91 eV at zero time to 458.65 eV after 24 h reaction. This small but significant shift indicates redox catalysis Ti^{4+}/Ti^{3+} taking place during the discoloration process involving two oxidation states.

3.3. Precluding the corrosion of cotton by TiO_2 by the use of SiO_2 as a binder

To avoid the corrosive action on the textile of the h^+ generated by TiO_2 under light, as shown below in reaction 1, SiO_2 layers were added on cotton having a large density of OH-groups/cm^2 compared to polyester and polyamide

$$h^+ + H_2O \rightarrow H^+ + OH^o \quad (1)$$

The amorphous TiO_2/SiO_2 layer in Fig. 5 presented sizes between 4 and 8 nm and had a width of 25 ± 10% nm. This is equivalent to 3–6 layers of TiO_2/SiO_2. The TiO_2 in a matrix of silica was effective in the

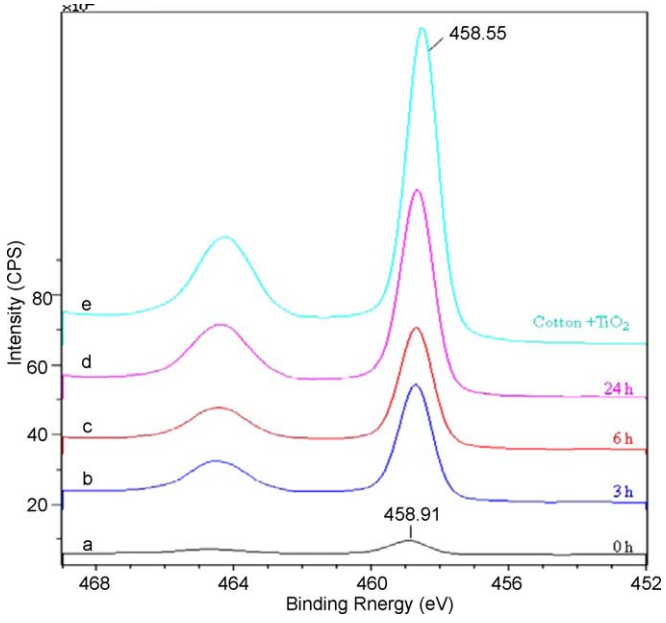

Fig. 4. XPS spectrum of Ti2p peaks of TiO_2-cotton stained with wine pretreated for 10 min by Vacuum-UV light, at atmospheric *P* and irradiated with Suntest light for: (a) 0 h, (b) 3 h, (c) 6 h, (d) 24 h (e) The TiO_2-coated cotton sample without wine was pretreated in the same way at zero time.

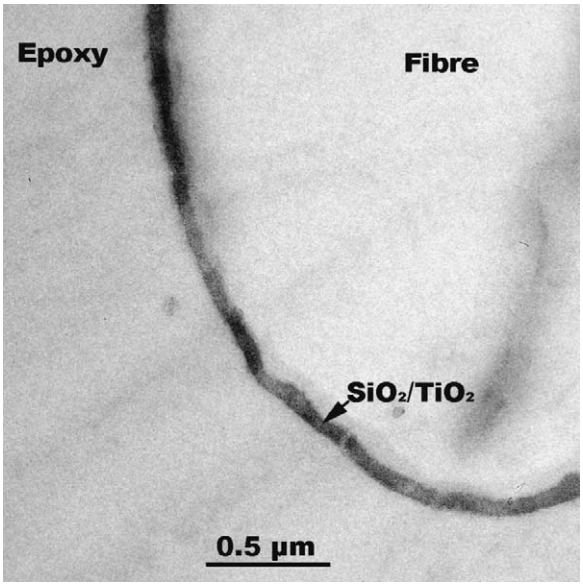

Fig. 5. Transmission electron microscopy of a sample of TiO_2/SiO_2 coated cotton.

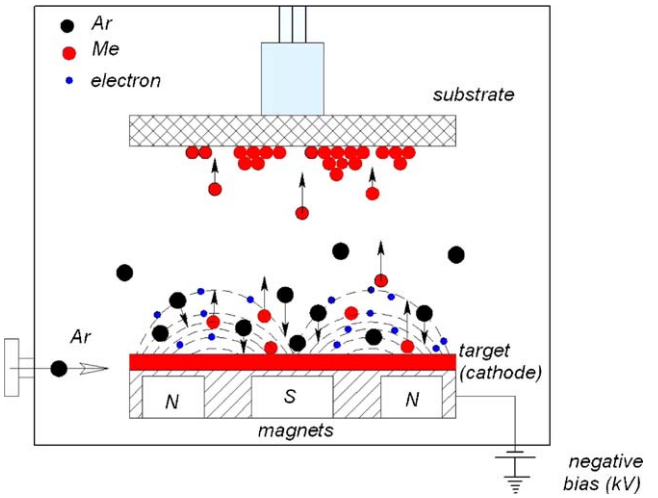

Fig. 6. Schematic diagram of the DC-magnetron sputtering unit. Me refer to the metal used as target and N and S stand for the poles in the magnetron unit.

wine stain discoloration and seems to preclude the corrosion of the fabric due to TiO_2 (h^+) [28]. The stained cotton was reused 6 times without decrease in the CO_2 evolution kinetics. After a sunlight irradiation period of 24 h, the TiO_2/SiO_2 layer presented the same structure and width as observed at time zero, proving the stable nature of the coating.

3.4. Biological inactivation of airborne bacteria on Ag-sputtered samples

Fig. 7a presents the photography of the non-sputtered cotton sample surrounded by a darker bacteria/*fungi* deposit. For Ag-cotton sputtered for 60 s and up to 600 s, the bacterial deposits do not appear around the dark Ag-loaded cotton borders (Fig. 7b). About 60 s sputtering time was necessary to deposit 0.0026 wt% Ag on the cotton as shown in Table 1. This was the Ag-threshold loading to make the cotton bactericide and inhibit bacterial/fungal after the incubation period as described in the Experimental section.

3.5. DC-sputtered Ag and Ag/Pt cotton samples

Fig. 8 shows the Ag-species on the cotton at DC-sputtering times between 15 and 600 s. Deposition times of 3, 7, 15, 30, 60 and 600 s lead to Ag and Ag/Pt layers of 4.6, 10.8, 23.3, 46.5, 93.0 and 930 nm thickness on the cotton surface [29–31]. Only cotton sputtered for 60 s or more showed bactericide effects on the airborne bacteria. This Ag threshold is equivalent to ~10 Ag-layers (40–50 nm) and is also the called the minimal inhibitory concentration (MIC). The 60 s sputtering time is short for making an economic use of Ag. The amount of Ag-ions on Ag-coatings has been reported to increase with increasing Ag-layer thickness on several substrates.

Samples of cotton loaded with Ag/Pt at 15, 60 and 600 s present an atomic surface concentration of 9.41, 18.46 and 35.28% of Ag along 0.12, 0.25 and 0.32% of Pt and were investigated to compare the Ag released with the Ag-species released from an Ag-target [29]. Three types of Ag were deposited by the magnetron unit as shown in Fig. 8 with Auger parameters at 725.15, 725.53 and 725.66 eV and are assigned to Ag^0, Ag^{+1} and Ag^{+2}, in sequential order. While the presence of Ag^0 and Ag^{+2} seems to be documented, the assignment to Ag^{+1} is less clear. The

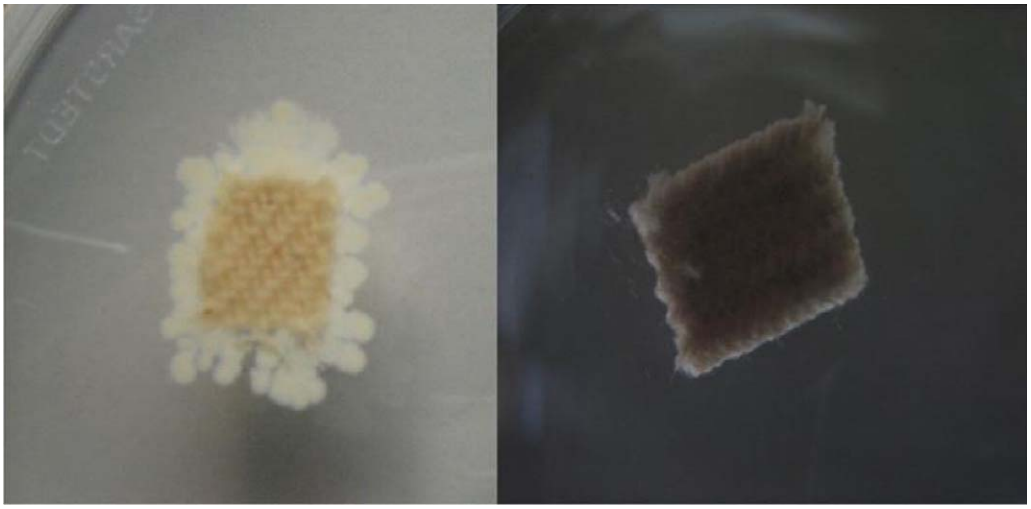

Fig. 7. (a) Non-sputtered cotton sample showing the growth of airborne bacteria after the incubation period. (b) Ag-sputtered cotton sample. The clear boundaries are due to the original color of the cotton fabric. No bacteria or fungi growth was observed.

Table 1
Ag and Pt-content of the cotton samples at different sputtering times determined by X-ray fluorescence.

Sample	Ag (wt%)	Pt (wt%)
Ag-Cotton 3 s	<0.001	<0.001
Ag-Cotton 15 s	0.0015	<0.001
Ag-Cotton 60 s	0.0026	<0.001
Ag-Cotton 600 s	0.0385	<0.001
Ag/Pt-Cotton 3 s	<0.001	<0.001
Ag/Pt-Cotton 15 s	0.0010	<0.001
Ag/Pt-Cotton 30 s	0.0034	0.0014
Ag/Pt-Cotton 60 s	0.0540	0.0073
Ag/Pt-Cotton 600 s	0.0630	0.0078
Cotton reference	<0.001	<0.001

Auger lines associated with XPS of Ag/cotton

Ag^0 725.15 eV

Ag(I) 725.53 eV

Ag(II)O 725.66 eV

Auger parameters for the Ag and Ag/Pt lines on cotton samples

Sputtering time	Cotton /Ag Auger parameter, α	Cotton /Ag/Pt Auger parameter, α
15 s	725.15	725.53
60 s	725.66	725.53
600 s	725.65	725.66

In the cotton Ag and in the cottonAg/Pt we have the same Ag-ionic species. No Galvanic effects due to pt wee observed after 60 s and up to 600s. This is the meaningful range of effective bactericide Ag surface concentration.

Fig. 8. Auger parameters for the different varieties of Ag deposited on cotton samples by DC-magnetron sputtering.

reason for that is that O 1s line at 530.71 results from the presence of two silver and platinum oxides and therefore, cannot be used for clear identification of the silver oxidation state. Silver XPS lines for the different oxidation states are well known for their poor chemical shift sensitivity <0.2 eV. For a quantitative evaluation we need to know exact position of each silver component with a precision >0.01 eV and this is not possible especially in the case of Ag^+. The striking observation is that the type of silver-ions produced using the Ag/Pt target is similar with the Ag target at each of the three sputtering times of 15, 60 and 600 s (Fig. 8). This explains the lack of an inhibitory effect of the Pt in the Pt/Ag target with respect to the Ag-target on the inactivation of airborne bacteria since in both cases similar Ag-ionic species were produced.

The Pt did not enhance the release of Ag-ions from the Ag/Pt target as expected from the higher position of Pt in the electrochemical/Galvanic scale respect to Ag. The Pt is above Ag in the galvanic scale and should enhance the formation of Ag-ions. This was not the case as shown by the data in Fig. 8. In the Galvanic scale the metal with a higher potential displace the metal at a lower position in the electrochemical scale upon contact generating metal ions. The Pt potential of −1.1 eV is higher than the Ag potential of −0.8 eV.

The adhesion of Ag to the cotton when using DC-magnetron sputtering was strong. Friction with paper or cloth did not allow smearing of the Ag. This is a major improvement respect to the adhesion of Ag-particle on cotton applied by reduction of colloidal Ag-salts as reported previously by our laboratory.

4. Conclusions

- Nanocrystalline anatase TiO_2 with small particles size distribution was synthesized and subsequently loaded on cotton and other fabrics activating previously activated by: (a) in air under RF-plasma at atmospheric pressure where heat effects were observed to break intermolecular H-bonding between the textile surface and –OH groups of adjacent molecules and (b) by pretreatment using Vacuum-UV (185 nm) also at atmospheric pressure allowed the formation of atomic O and excited O^* in the gas phase due to the extremely low molecular optical absorption of O_2 and N_2 at 185 nm.
- Good reproducibility for the discoloration was obtained in both cases for red wine stains under simulated solar light. A more uniform coating of TiO_2 on cotton was obtained retreating with UVC as compared to RF.
- In the ongoing work with Ag-textiles directed towards the deposition of transparent, thin, highly adhesive Ag-layers of any shape on fabrics, the sputtering from an Ag-target for 60 s led to thin semi-transparent coatings. This coating consisted of with 4–5 Ag-layers and showed strong adherence and bactericide activity. The Ag-coating did not affect the flexibility/handling of the textile.

Acknowledgments

We thank the COST Action 540 PHONASUM "Photocatalytic technologies and novel nanosurface materials, critical issues" and COST Action MP0804 "Highly Ionized Pulse Plasma Processes" for the financial support for this study.

References

[1] A. Bozzi, T. Yuranova, J. Kiwi, Self-cleaning of wool-polyamide and polyester textiles due to surfaace-TiO_2 rutile modification under daylight irradiation, J. Photochem. Photobiol. A 172 (2005) 27–34.
[2] A. Bozzi, T. Yuranova, I. Guasaquillo, D. Laub, J. Kiwi, Self-cleaning of cotton textiles modified with TiO_2 at low temperatures under daylight irradiation, J. Photochem. Photobiol. A. 174 (2005) 156–164.
[3] T. Yuranova, R. Mosteo, J. Bandara, D. Laub, J. Kiwi, Cotton textiles modified by SiO_2/TiO_2 with self-cleaning properties, J. Mol. Catal. A 244 (2006) 160–167.
[4] M.I. Mejía, J.M. Marín, G. Restrepo, C. Pulgarín, E. Mielczarski, J. Mielczarski, Y. Arroyo, J.-C. Lavanchy, J. Kiwi, Preparation, testing and performance of TiO_2/Polyester for the degradation of gaseous methanol, Appl. Catal. B 91 (2009) 481–488.
[5] M.I. Mejía, J.M. Marín, G. Restrepo, C. Pulgarín, E. Mielczarski, J. Mielczarski, J. Kiwi, Magnetron-sputtered Ag-modified cotton textiles active in the inactivation of airborne bacteria accepted, ACS Appl. Mater. Interf. (2010).
[6] A.W. Daoud, S.K. Leung, W.S. Tung, J.H. Xin, K. Cheuk, K. Qi, Self-cleaning keratins, Chem. Mater. (2008), 1242–121254.
[7] W. Daoud, H. Xin, Synthesis of single-phase nanocrystallites at room temperature, Chem. Comm. (2005) 2110–2112.
[8] W.S. Tung, W.A. Daoud, Photocatalytic self-cleaning keratins. A feasibility study, Acta Biomater. 5 (2009) 53–56.
[9] W.A. Daoud, J.H. Xin, Nuleation and growth of anatase crystallites on cotton fabrics a low temperature, J. Am. Ceram. Soc. 87 (2004) 953–955.
[10] W.S. Tung, W.A. Daoud, Effect of wettability and silicon surface modification on self-cleaning functionalization of wool, J. Appl. Polym. Sci. 12 (2009) 235–243.
[11] M. Radetic, V. Ilic, V. Vodnik, S. Dimitijevic, P. Jovancic, Z. Saponjic, J. Nedeljkovic, Antibacterial effect of silver nanoparticles deposited on corona-treated polyester and polyamide fibers, Polym. Adv. Technol. 19 (2008) 1816–1821.
[12] M. Montazer, M.G. Afgeh, X-Linking and Antimicrobial finishing of cotton fabric, J. Appl. Polym. Sci. 103 (2007) 178–185.
[13] R. Dastjerdi, M. Montazer, S. Shahsavan, A new method to stabilize nanoparticles on textile surfaces, Colloid Surf. A: Physicochem. Eng. Aspects 345 (2009) 202–210.
[14] D. Hegemann, M. Amberg, A. Ritter, M. Heuberger, Recent developments in Ag-metallised textile plasma sputtering, Mats. Technol. 24 (2009) 41–45.
[15] L. Geranio, M. Heuberger, B. Nowack, The behavior of silver nanotextiles during washing, Environ. Sci. Technol. 43 (2009) 8113–8118.
[16] M. Amberg, K. Greder, M. Barbadoro, M. Heureberg, D. Hegemann, Electrochemical behavior of nanoscale Ag-coatings on PET fibers, Plasma Proc. Polym. 5 (2008) 874–880.
[17] A. Ritter, F.A. Reifler, S. Saini, Quick screening method for the photocatlytic activity of nanoparticles powder materials, Appl. Catal. A 35 (2008) 271–276.

[18] D. Hegemann, M.M. Hossain, D. Balazs, Nanostructured plasma coatings to obtain multifunctional textile surfaces, Prog. Org. Coat. 58 (2007) 237–240.
[19] N. Abidi, E. Hequet, S. Tarimala, L.L. Dai, Cotton fabric surface modification for UV-protection using sol–gel methods, J. Appl. Polym. Sci 104 (2007) 111–117.
[20] R.H. Wang, J.H. Xin, Y. Yang, F.H. Liu, M.L. Xu, J.H. Xu, The characteristics and photocatalytic activities of silver doped ZnO nanocrystalls, Appl. Surf. Sci. 227 (2004) 312–317.
[21] M.C. Long, W.M. Cai, J. Cai, B.X. Zhou, Y. Chai, Y.H. Wu, Efficient degradation of phenol over $Co_3O_4/BiVO_4$ under visible light, J. Phys. Chem. B 110 (2006) 20211–20216.
[22] M. Jin, X. Zhang, S. Nishimoto, Z. Liu, D. Tryk, A. Emeline, T. Murakami, A. Fujishima, Light-stimulated composition conversion in TiO_2 based nanofibers, J. Phys. Chem. C 111 (2007) 658–665.
[23] J. Kasanen, M. Suvanto, T.T. Pakkanen, Self-cleaning TiO_2 multilayer coatings fabricated by polymer glass, J. Appl. Polym. Sci. 111 (2009) 2597–2602.
[24] A.G. Rincon, C. Pulgarin, Use of a coaxial photocatlytic reactor (CAPHORE) on the photoassisted treatment of mixed *E coli* and Bacillus *sp* and bacterial community present on waste waters, Catal. Today 101 (2005) 331–344.
[25] M. Radetic, personal communication (2009).
[26] M. Dhananjeyan, J. Kiwi, R. Thampi, Performance of titania and iron oxide immobilized on derivatized polymer films for mineralization of pollutants, Chem. Commun. (2000) 1443–1444.
[27] K. Meilert, D. Laub, J. Kiwi, Photocatalytic self-cleaning of modified cotton textiles by TiO_2 clusters attached by chemical spacers, J. Mol. Catal. A 237 (2005) 101–108.
[28] T. Yuranova, A.G. Rincon, D. Laub, J. Kiwi, Synthesis, activity and characterization of textiles showing self-leaning and bactericidal activity, Catal. Today 122 (2007) 109–117.
[29] M.I. Mejía, G. Restrepo, J.M. Marín, R. Sanjines, C. Pulgarín, E. Mielczarski, J. Mielczarski, J. Kiwi, Magnetron-sputtered Ag-modified cotton textiles active in the inactivation of airborne bacteria, ACS Appl. Mater. Interf. 2 (2010) 230–235.
[30] T Yuranova, A.M. Rincon, A. Bozzi, S. Parra, C. Pulgarin, J. Kiwi, Antibacterial textiles prepared by RF-plasma and vacuum-UV mediated deposition of silver, J. Photochem. Photobiol. A. 161 (16) (2003) 27–34.
[31] T. Yuranova, A.M. Rincón, C. Pulgarin, D. Laub, N. Xanthopoulos, J.-H. Mathieu, J. Kiwi, Bactericide cotton textiles active in *E coli* abatement prepared under mild preparation conditions, J. Photochem. Photobiol. A. 181 (2006) 363–369.